Journal of ELECTRONIC MATERIALS, Vol. 45, No. 8, 2016
DOI: 10.1007/s11664-016-4604-4

Charge Carrier Relaxation Study in Glass-Added Barium Titanate Ceramics Using Thermally Stimulated Depolarization Current

QIAN ZHANG,[1,2] YONG ZHANG,[1,4] XIAOLIN LIU,[2] XIAOZHEN SONG,[1] JIA ZHU,[1] and IVAN BATURIN[3]

1.—Beijing Key Laboratory of Fine Ceramics, State Key Laboratory of New Ceramics and Fine Processing, Institute of Nuclear and New Energy Technology, Tsinghua University, Beijing 100084, People's Republic of China. 2.—State Key Laboratory of Organic-Inorganic Composites, Beijing University of Chemical Technology, Beijing 100029, People's Republic of China. 3.—Ferroelectric Laboratory, Institute of Natural Science, Ural Federal University, Ekaterinburg 620000, Russia. 4.—e-mail: yzhang@tsinghua.edu.cn

The depolarization process of glass-added barium titanate ($BaTiO_3$) ceramics with two different glass concentrations was investigated using a thermally stimulated depolarization current (TSDC) technique. The TSDC spectra of the glass-added $BaTiO_3$ ceramics show three peaks. The first sharp peak near the Curie temperature is due to pyroelectric current associated with ferroelectric-paraelectric phase transition. The middle temperature peak at about 200°C showed no dependence on polarization field, and the activation energies of this peak were between 0.43 eV and 0.55 eV, which are attributed to the behavior of defect dipoles related to oxygen vacancies within the $BaTiO_3$ grains. Moreover, the high temperature peak at around 300°C indicated that the depolarization current peak position depends on the polarization temperature and decreases with increasing polarization field. The activation energy of this high temperature peak was between 0.78 eV and 0.98 eV, which is similar to the activation energy for the motion of oxygen vacancies in perovskite oxides. The high temperature peak could be attributed to the migration of oxygen vacancies across grain boundaries. In this work we developed a model in which oxygen vacancies that originated from the defect within grains migrated from the anode to the cathode and some were trapped at the grain boundaries. It is presented here and successfully interprets the appearance and behavior of these peaks.

Key words: Oxygen vacancy, barium titanate ceramics, activation energy, thermally stimulated depolarization current

INTRODUCTION

Barium titanate ($BaTiO_3$) ceramics have diverse applications in multilayer ceramic capacitors (MLCC),[1] electro-optic devices,[2] and thermistors.[3] Conventional $BaTiO_3$ ceramics require a high sintering temperature. This requirement is an apparent barrier in developing dielectric materials for MLCC applications. Glasses such as ZnO-B_2O_3-SiO_2,[4] PbO-B_2O_3,[5] and BaO-B_2O_3-SiO_2[6] have been utilized as additives in $BaTiO_3$ ceramics and thick films to reduce the sintering temperature. The increase of dielectric breakdown strength and the reduction of grain size have been documented for the case of specific glass-added $BaTiO_3$ ceramics with increasing glass content.[7] Also, a substantial improvement in voltage endurance was demonstrated experimentally

(Received September 13, 2015; accepted April 28, 2016; published online May 11, 2016)

in these glass-added $BaTiO_3$ ceramics.[8] The increase in the observed dielectric breakdown strengths could be due to three factors: (i) the reduction of grain size, (ii) the reduction of internal field, and (iii) changes in space charge distribution.[9]

In order to obtain a better understanding of the space charge role in the process of dielectric breakdown, lifetime behavior and charge carrier relaxation need to be investigated. A considerable amount of attention has been given to the presence of charge carriers in the glass-added $BaTiO_3$ ceramics and the possible role of such carriers in the electrical behavior. Various characterization techniques were utilized in an attempt to determine the dielectric relaxation processes. Impedance spectroscopy has been recognized as a powerful technique to distinguish various conductivity contributions such as grain, grain boundary, and electrode/dielectric interface of many oxide ceramic materials that possess ionic or mixed ionic-electronic conduction.[10,11] An alternative approach to studying the dielectric relaxation is based on thermally stimulated depolarization current (TSDC). TSDC measurement may provide complementary information about the type of defects existing in the materials such as dipole, trap charge, and space charge,, as well as the quantification of these defects, and thus could enable a better understanding of the physical phenomena related to such defects.[12,13] In general, TSDC consists of the poling of the sample at elevated temperature followed by recording the depolarization current flowing through the ammeter during the linear increase of temperature. Due to a relatively simple experimental setup and high resolution, TSDC has been widely used to study dipole relaxation, charge storage, and charge decay processes in polymer dielectrics[14–17] as well as in ceramic dielectrics.[12,13,18–21] The type of charge carriers can be determined through polarization temperature T_p and polarization field E_p dependencies of the depolarization current peak position T_m.[14,18] Electronic and ionic polarization mechanisms are independent of T_p, whereas the dipolar and space charge polarizations are dependent on T_p.

In this work, the dielectric relaxation of the $BaTiO_3$ ceramics with different glass concentrations was characterized using the TSDC method. This study extends our previous work[7] to understand the charge carrier relaxation in glass-added $BaTiO_3$ ceramics. An attempt is made to explain the TSDC spectra with an emphasis on the defect migration in conjunction with the change of polarization conditions.

MATERIALS AND METHODS

Hydrothermally derived barium titanate ($BaTiO_3$) powder used in this study was supplied by Guoteng Co. Ltd., Shandong, China, and its average particle size was approximately 100 nm. The composition of the specific glass employed is 27.68BaO-6.92SrO-29TiO_2-22SiO_2-12Al_2O_3-2.4BaF_2 (mol.%). The fabrication of this glass and the synthesis of the glass-added $BaTiO_3$ ceramics have been reported before.[7] The $BaTiO_3$ ceramics with 5 wt.% and 7 wt.% glass additions were chosen for the present study. Prior to the measurements, a silver paste was screen-printed on both surfaces of the ceramics and subsequently fired in air at 550°C for 30 min.

The glass-added $BaTiO_3$ ceramics were thermally etched for 15 min at 1130°C after being polished. These thermal-etched specimens were examined using field emission scanning electron microscopy (Model Quanta 200 FEG, FEI, Eindhoven, the Netherlands). TSDC measurements were performed using a pA meter (4140B, Hewlett Packard, Palo Alto, CA) controlled by the LabVIEW program. The schematic diagrams of polarization and the heating profile of TSDC measurement have been reported elsewhere.[22] During the polarization procedure, the samples were heated to a polarization temperature T_p, and then a dc polarization field E_p was applied for 30 min. The samples were then rapidly cooled to a starting temperature T_o (0°C), maintaining the polarization field E_p. The samples were then short-circuited by setting E_P to zero. The depolarization currents were then measured while the samples were being heated up to 400°C at a constant heating rate β of 3°C/min.

RESULTS AND DISCUSSION

Microstructure of the Glass-Added $BaTiO_3$ Ceramics

In Fig. 1, the SEM micrographs of polished and thermally etched surfaces of $BaTiO_3$ ceramics added with different glass concentrations are presented. These samples were sintered at 1180°C for 2 h. The average grain size has been obtained by image analysis techniques. It was reported here with an accuracy of ±5% at a 95% confidence level. As shown in Fig. 1, the average grain size of the 5 wt.% glass-added $BaTiO_3$ ceramics is about 0.60 μm, while it decreases to about 0.46 μm for the 7 wt.% glass-added $BaTiO_3$ ceramics. Moreover, the specimen exhibits a homogeneous microstructure with the obvious gaps between crystalline grains.

TSDC Spectra of the Glass-Added $BaTiO_3$ Ceramics

The typical TSDC spectra of the $BaTiO_3$ ceramics with different glass additions are shown in Fig. 2. During these measurements the polarization field E_P and the polarization temperature T_P were fixed to 120 V/mm and 260°C, respectively. It is evident that the TSDC spectra were composed of three peaks. The first peak, A, appears at 130°C, the second peak, B, at 200°C, and the third peak, C, is at 300°C. The sharp peak A that appears near the

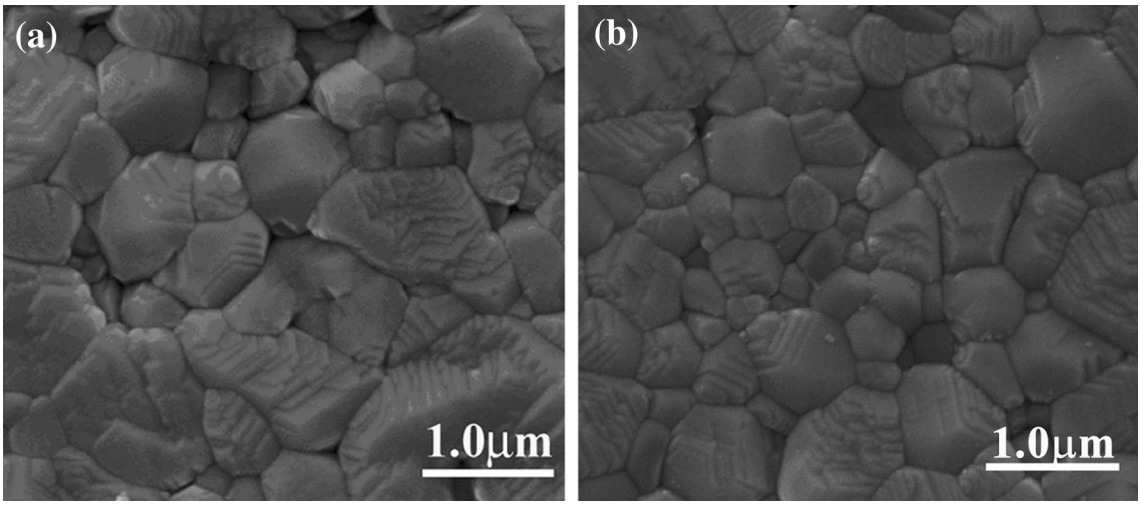

Fig. 1. SEM micrographs of the $BaTiO_3$ ceramics with different glass concentrations: (a) 5 wt.%, (b) 7 wt.%. The samples were thermally etched for 15 min at 1130°C after being polished.

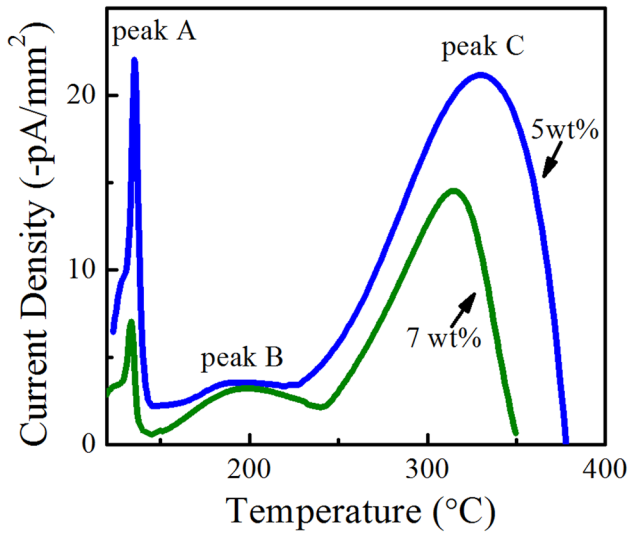

Fig. 2. TSDC spectra of the $BaTiO_3$ ceramics with different glass concentrations.

Curie temperature is due to the pyroelectric current associated with the ferroelectric-paraelectric phase transition, which is in good agreement with previous studies on pure $BaTiO_3$.[23] In addition, comparisons of the TSDC spectra taken on the glass-added $BaTiO_3$ ceramics revealed that the intensities of the peaks decrease with the increase of glass concentration.

In order to explain the TSDC spectra of these $BaTiO_3$ ceramics with different glass concentrations, a simple brick wall model with ordered cubic grains and consequently regular grain boundaries was employed to calculate the thickness of the glassy grain boundary. Assuming that the bulk densities of the $BaTiO_3$ phase and the glassy phase are 6.08 g/cm^3 and 4.1 g/cm^3, respectively, the volume fraction of the glass phase in the 5 wt.% and 7 wt.% glass-added $BaTiO_3$ ceramics was derived to be 7 vol.% and 10 vol.%, respectively. With such a hypothesis, we can proceed to analyze the thickness of the glassy grain boundary in the ceramics. The estimated average thicknesses of glassy gaps between crystalline grains are 15.0 nm for the 5 wt.% glass-added $BaTiO_3$ ceramics and 16.5 nm for the 7 wt.% glass-added $BaTiO_3$ ceramics. Therefore, the actual electric field within grains in the 5 wt.% glass-added $BaTiO_3$ ceramics is higher than that in the 7 wt.% glass-added $BaTiO_3$ ceramics. Then, the value of the peak current density J_m in the 5 wt.% glass-added $BaTiO_3$ ceramics should be higher if the applied voltage and sample thickness were to be kept constant.

Calculation of Activation Energy

Bucci and Fieschi[24] firstly developed a model to quantitatively study the TSDC thermogram, in which the relaxation time $\tau(T)$ obeys an Arrhenius equation (first-order rate process).

$$\tau(T) = \tau_0 \exp\left(\frac{E_a}{kT}\right) \tag{1}$$

where τ_0 is a pre-exponential factor, E_a is the activation energy, k is the Boltzmann constant, and T is the absolute temperature. The simplest kinetics, which describe the dipole relaxation process, has been successfully used to explain the temperature dependence of TSDC.[15,25]

$$I(T) = \frac{P_0}{\tau_0}\exp\left[-\frac{E_a}{kT} - \frac{1}{\beta\tau_0}\int_{T_0}^{T}\exp\left(-\frac{E_a}{kT'}\right)dT'\right] \tag{2}$$

where $I(T)$ is the current intensity at temperature T with a constant heating rate β, and P_0 is initial polarization intensity. Its value could be calculated using the following formula:

$$P_0 = N\mu^2 E_p \alpha / kT_p \quad (3)$$

where α is the geometrical factor depending on the possible dipolar orientation, and for nearest-neighbor face-centered vacancy positions in ionic crystals, $\alpha = 2/3$, N is the concentration of dipoles, μ is the electrical dipole moment. Therefore, the maximum peak current density J_m at the temperature T_m should intensify linearly with the increase of polarization field E_p. By differentiating Eq. 2, the maximum temperature T_m corresponding to the peak current position can be obtained.

$$T_m^2 = \frac{E_a}{k}\beta\tau_0 \exp\left(\frac{E_a}{kT_m}\right) \quad (4)$$

From the above Eq. 4, it is readily seen that for a given heating rate β, it will have a fixed value of T_m. That is to say, polarization field has no effect on the temperature T_m but it does have a linear effect on peak current density J_m of the dipole depolarization peak.

An area method[26,27] was used to calculate the activation energy of peaks for the glass-added $BaTiO_3$ ceramics shown in Fig. 2. Since the depolarization current density $J(T)$ is the decreasing rate of the polarization,

$$J(T) = \frac{I(T)}{A} = -\frac{dP(T)}{dt} = -\beta\frac{dP(T)}{dT} \quad (5)$$

where A is the effective area of the electrodes, $P(T)$ is the remaining polarization at temperature T. Based on the assumption that the decay of the polarization with time ($\beta = dT/dt$) is a first-order rate process, the elementary single motional process is expressed by:

$$\frac{dP(T)}{dt} = -\frac{P(T)}{\tau(T)} = \frac{\beta dP(T)}{dT} \quad (6)$$

Combining Eqs. 5 and 6, it comes out that

$$\tau(T) = \frac{P(T)}{J(T)} \quad (7)$$

Now, the residual polarization $P(T)$ at temperature T is given by

$$P(T) = \frac{1}{\beta}\int_T^\infty J(T)dT \quad (8)$$

According to Eqs. 7 and 8, $\tau(T)$ is indicated by

$$\tau(T) = \frac{1}{J(T)\beta}\int_T^\infty J(T)dT \quad (9)$$

From Eqs. 1 and 9,

$$\ln[\tau(T)] = \frac{E_a}{kT} + \ln(\tau_0) \quad (10)$$

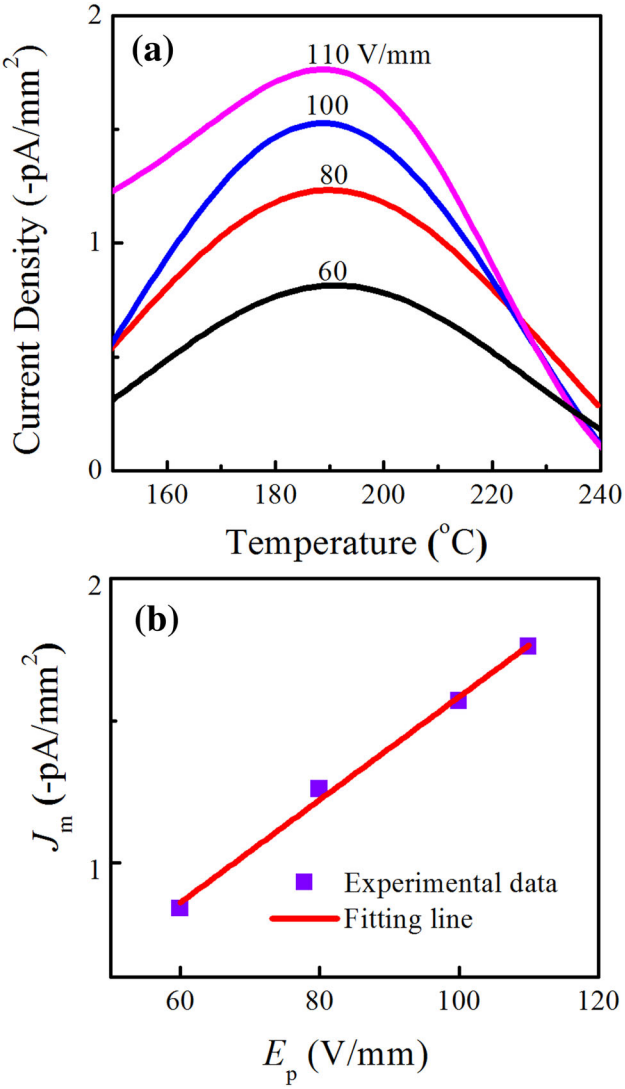

Fig. 3. (a) TSDC spectra of 7 wt.% glass-added $BaTiO_3$ ceramics polarized at various polarization fields from 60 V/mm to 110 V/mm at T_p = 180°C, (b) Polarization field E_p dependence of J_m for peak B.

Effect of Polarization Conditions on Peak B

Figure 3a depicts a series of TSDC spectra near peak B obtained from the 7 wt.% glass-added $BaTiO_3$ ceramics that are polarized with various polarization fields ranging from 60 V/mm to 110 V/mm at T_p = 180°C. The peak current density J_m of the peak B shows a linear increase with the increase of E_p (see Fig. 3b), while T_m is fixed, as shown in Fig. 3a. This result is consistent with the Bucci-Fieschi theory, which indicates that this peak is related to the relaxation of dipoles. This is further verified by the T_p dependence of T_m for peak B (Fig. 4). It was shown that the T_m for peak B shifted to lower temperatures with increasing polarization temperature at E_p = 120 V/mm.

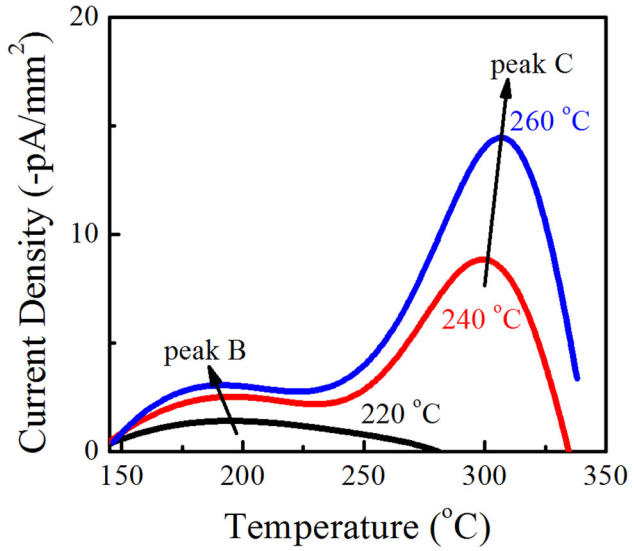

Fig. 4. TSDC spectra of the 7 wt.% glass-added $BaTiO_3$ ceramics polarized at various polarization temperatures from 220°C to 260°C at E_p = 120 V/mm.

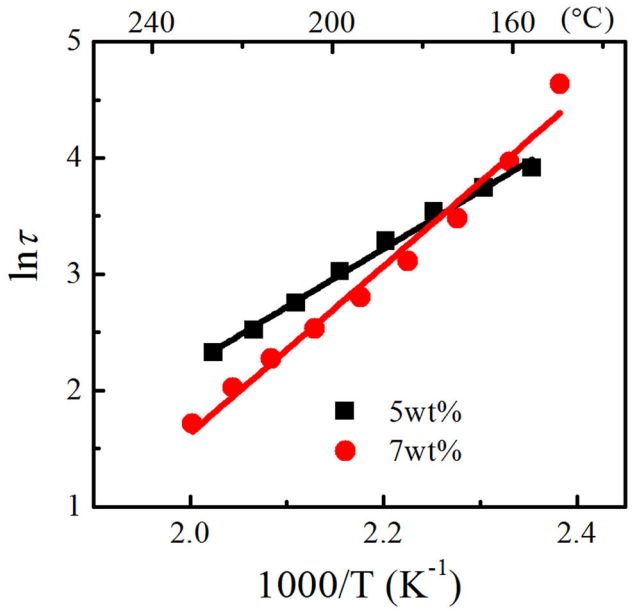

Fig. 5. An ln τ versus 1/T Arrhenius plot for peak B.

Figure 5 shows the values of the activation energy obtained from the slope of lnτ as a function of 1/T. The plot indicates that a single relaxation process contributes to peak B. The activation energy of peak B slightly changes between 0.43 eV and 0.55 eV, which is in the range of 0.3–0.6 eV of the dipolar activation energy in the $BaTiO_3$ ceramic system.[28]

Effect of Polarization Conditions on Peak C

Figure 6 shows TSDC spectra for the $BaTiO_3$ ceramics with 5 wt.% glass concentration. In these

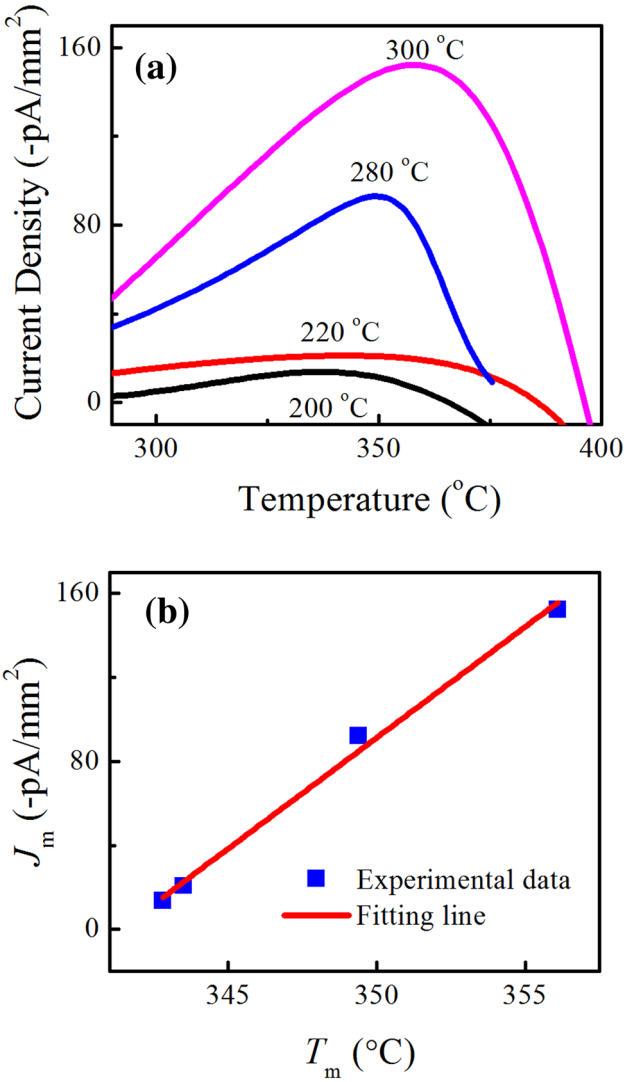

Fig. 6. (a) TSDC spectra of the 5 wt.% glass-added $BaTiO_3$ ceramics polarized at various polarization temperatures from 200°C to 300°C at E_p = 120 V/mm, (b) T_m dependence of J_m for peak C.

measurements, polarization field E_p was fixed to 120 V/mm and polarization temperature T_p was varied. It is found that the T_m for peak C shifts from 342°C to 356°C and J_m increases from 13.5 pA/mm^2 to 152 pA/mm^2 when the T_p is increased from 200°C to 300°C. Figure 6b shows the dependence of J_m on T_m for this composition. A linear relationship was observed over the studied polarization temperature range. Such behavior is a typical characteristic of space charge polarization. TSDC spectra for the $BaTiO_3$ ceramics with 5 wt.% glass addition obtained under fixed T_p = 300°C and varying polarization field E_p are shown in Fig. 7. The decrease of T_m and the increase of J_m with increasing E_p were observed. It can be concluded from these data that peak C can be attributed to the detrapping of space charge.[18]

The lnτ versus 1/T plot for peak C was shown in Fig. 8. The activation energy for peak C was

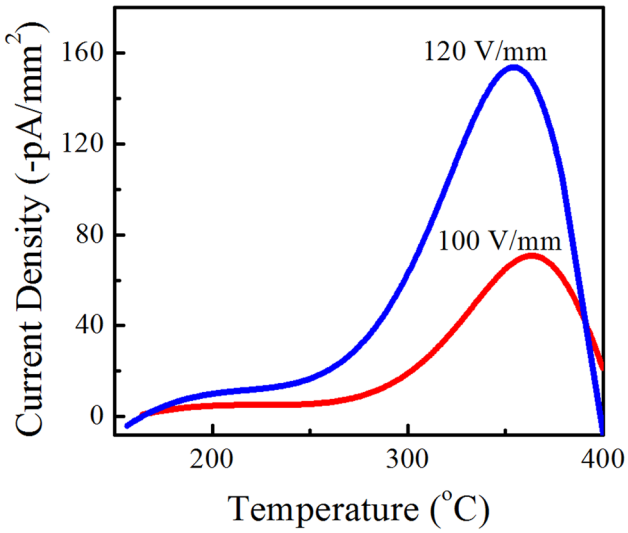

Fig. 7. TSDC spectra of the 5 wt.% glass-added $BaTiO_3$ ceramics polarized at various polarization fields from 100 V/mm to 120 V/mm at T_p = 300°C.

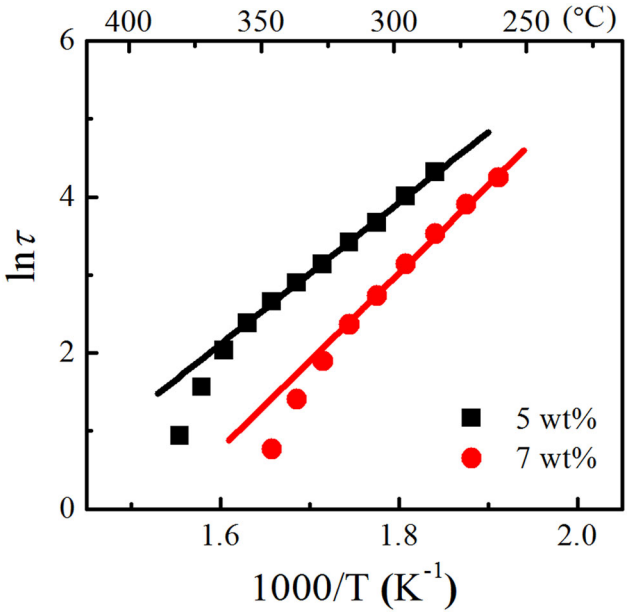

Fig. 8. An ln τ versus 1/T Arrhenius plot for peak C.

calculated from Fig. 8. For the 5 wt.% and 7 wt.% glass additions, while the activation energies were 0.78 eV and 0.98 eV, respectively. These values are similar to the activation energies (0.7–1.1 eV) for the motion of oxygen vacancies in perovskite oxides previously determined by impedance spectroscopy.[29,30]

Model and Mechanisms

It is well known that the generation of oxygen vacancies in $BaTiO_3$ ceramics could be due to the high temperature treatment and/or the substitution of an acceptor oxide, according to Eqs. 11 and 12:

$$2O_O^{\times} \rightarrow O_2(g) + 2V_O^{\cdot\cdot} + 4e' \quad (11)$$

$$Al_2O_3 \xrightarrow{TiO_2} 2Al'_{Ti} + V_O^{\cdot\cdot} + 3O_O^{\times} \quad (12)$$

Among various types of defects in $BaTiO_3$ ceramics, oxygen vacancies will be rather mobile because there are always nearest-neighbor oxygen sites in the perovskite structure with which the oxygen vacancies may exchange its position.[31,32] More mobile oxygen vacancies would be attracted and swing around the vicinity of the oppositely charged center, which results in the formation of defect complexes such as $(Al'_{Ti} - V_O^{\cdot\cdot})^{\cdot}$. These defect complexes would break up with increasing temperature and the dissociated oxygen vacancies could cause the long range relaxation. Moreover, the diffusion of oxygen vacancies can also be hindered by grain boundaries.[33] Based on the above results, we proposed a model for explaining the TSDC spectra. As shown in Fig. 9, two kinds of oxygen vacancies in the glass-added $BaTiO_3$ ceramics are illustrated. One kind of oxygen vacancy migrates within the grains, while another kind of oxygen vacancy transports across the grain boundaries. At the beginning of polarization, oxygen vacancies are randomly distributed in the sample, as seen in Fig. 9a. Peak B originates from the orientation of defect dipoles, and the most probable dipole caused by acceptor doping in our sample is $(Al'_{Ti} - V_O^{\cdot\cdot})^{\cdot}$, which results in the in-grain relaxation of defect dipoles that accumulate at the cathode side of the grain boundaries during polarization (in Fig. 9b). Peak C is assigned to the long-range relaxation due to the migrated oxygen vacancies across grain boundaries, which would be depleted in the anodic region and piled-up in the cathode region after polarization (in Fig. 9c). The correlation of peak C with the migration across the grain boundaries of oxygen vacancies could be explained by the occurrence of peak temperature, which is in the range of 300°C to 400°C.

When a weak polarization condition is selected, the relaxation of these oxygen vacancies inside each grain gives only peak B (in Fig. 3a). With the increase of T_p, the mobility of oxygen vacancies increases and some oxygen vacancies start to migrate across the grain boundaries and transport into the next grain, which leads to the presence of peak C at higher temperatures. Meanwhile, peak C is significantly smaller (in Fig. 4, T_p = 220°C) due to the incomplete polarization of the migrated oxygen vacancies across grain boundaries. As the T_p and E_p were increased, the J_m of peak C continued to increase, suggesting higher concentrations of oxygen vacancies are accumulated close to the cathode region, as shown in Figs. 6a and Fig. 7. In addition, the disappearance of peak B observed in Fig. 7 is due to the strong polarization condition which will

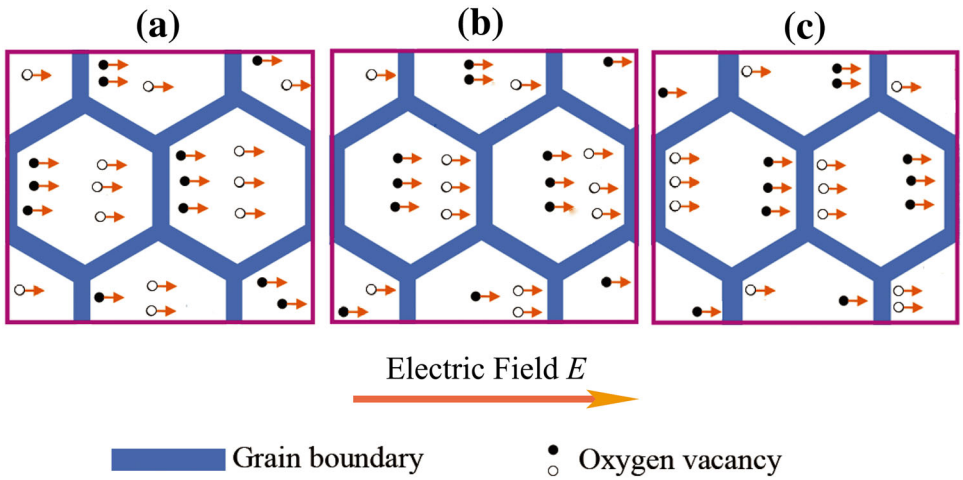

Fig. 9. The schematic diagram of the spatial profile of oxygen vacancy in the initial state (a), polarized under a weak polarization condition (b), and under a strong polarization condition (c). Two kinds of oxygen vacancies in the glass-added $BaTiO_3$ ceramics: solid circles represent oxygen vacancies migrated within the grains, while open circles represent oxygen vacancies transported across the grain boundaries.

decrease the contribution of in-grain defect dipole relaxation. Therefore, it is important to select proper polarization conditions for ensuring that the desired current peaks can be obtained in an TSDC experiment. In our measurements, only when E_P reaches 120 V/mm and T_P reaches 260°C could both peaks B and C be clearly observed, as shown in Fig. 2.

CONCLUSION

Thermally stimulated depolarization current measurements were carried out in $BaTiO_3$ ceramics with two different glass concentrations to investigate the charge carrier relaxation behavior. The TSDC spectra are composed of three peaks in the temperature range from 100°C to 350°C. For the middle-temperature peak that appeared at about 200°C, its peak position is independent of the polarization field. The physical origin of its relaxation was linked to the behavior of defect dipoles within the grain. In the case of the high-temperature peak at more than 300°C, its peak position has polarization temperature dependence, and decreases with increasing polarization field. This peak was ascribed to the migration of oxygen vacancies across grain boundaries. A model was proposed to explain the observed TSDC spectra.

ACKNOWLEDGEMENTS

This work was supported by the International Science & Technology Cooperation Program of China (No. 2012DFR50560) and the National Natural Science Foundation of China (Grant No. 51372014).

REFERENCES

1. M.J. Pan and C.A. Randall, *IEEE Electr. Insul. Mag.* 26, 44 (2010).
2. P. Tang, D. Towner, A. Meier, and B. Wessels, *Appl. Phys. Lett.* 85, 4615 (2004).
3. Y.M. Chiang and T. Takagi, *J. Am. Ceram. Soc.* 73, 3286 (1990).
4. H.I. Hsiang, C.S. Hsi, C.C. Huang, and S.L. Fu, *J. Alloy. Compd.* 459, 307 (2008).
5. S.F. Wang, T.C. Yang, Y.R. Wang, and Y. Kuromitsu, *Ceram. Int.* 27, 157 (2001).
6. H.P. Jeon, S.K. Lee, S.W. Kim, and D.K. Choi, *Mater. Chem. Phys.* 94, 185 (2005).
7. X.R. Wang, Y. Zhang, X.Z. Song, Z.B. Yuan, T. Ma, Q. Zhang, C.S. Deng, and T.X. Liang, *J. Eur. Ceram. Soc.* 32, 559 (2012).
8. A. Young, G. Hilmas, S.C. Zhang, and R.W. Schwartz, *J. Am. Ceram. Soc.* 90, 1504 (2007).
9. M. Touzin, D. Goeuriot, C. Guerret Piécourt, D. Juvé, and H.J. Fitting, *J. Eur. Ceram. Soc.* 30, 805 (2010).
10. R. Gerhardt, *J. Phys. Chem. Solids* 55, 1491 (1994).
11. C. Elissalde and J. Ravez, *J. Mater. Chem.* 11, 1957 (2001).
12. S.H. Yoon, C.A. Randall, and K.H. Hur, *J. Am. Ceram. Soc.* 92, 1766 (2009).
13. W. Liu and C.A. Randall, *J. Am. Ceram. Soc.* 91, 3251 (2008).
14. L. Gong, X. Zhang, Y. Shi, and L. Zhang, *Polym. Bull.* 68, 847 (2012).
15. Y. Shi, X.Y. Zhang, and L.L. Gong, *Polym. Bull.* 67, 1595 (2011).
16. E. Kim, T. Takeda and Y. Ohki, *IEEE Trans. Dielect. Electr. Insul.* 3, 386 (1996).
17. P. Raj, S. Lal, S. Mahna, and J. Quamara, *Int. J. Polym. Anal. Ch.* 17, 235 (2012).
18. H. Lee, J.R. Kim, M.J. Lanagan, S. Trolier Mckinstry, and C.A. Randall, *J. Am. Ceram. Soc.* 96, 1209 (2013).
19. S.H. Yoon, C.A. Randall, and K.H. Hur, *J. Am. Ceram. Soc.* 93, 1950 (2010).
20. N. Bogris, J. Grammatikakis, and A. Papathanassiou, *Phys. Rev. B* 58, 10319 (1998).
21. F. El Kamel, P. Gonon, F. Jomni, and B. Yangui, *J. Appl. Phys.* 100, 054107 (2006).
22. Z.L. Zhao, Y. Zhang, Q. Zhang, X.Z. Song, J. Zhu, X.R. Wang, and Z.Q. Zheng, *Phys. Status Solidi A* 211, 2150 (2014).
23. J. Jeong and Y.H. Han, *J. Electroceram.* 17, 1051 (2006).
24. C. Bucci and R. Fieschi, *Phys. Rev. Lett.* 12, 16 (1964).
25. N. Horiuchi, M. Nakamura, A. Nagai, K. Katayama, and K. Yamashita, *J. Appl. Phys.* 112, 074901 (2012).
26. J.J. Moura Ramos and N.T. Correia, *Thermochim. Acta* 426, 185 (2005).
27. S. Nakamura, H. Takeda, and K. Yamashita, *J. Appl. Phys.* 89, 5386 (2001).

28. S.H. Cha and Y.H. Han, *J. Appl. Phys.* 100, 104102 (2006).
29. A. Chen, Y. Zhi, and L. Cross, *Phys. Rev. B* 62, 228 (2000).
30. W.L. Warren, K. Vanheusden, D. Dimos, G.E. Pike, and B.A. Tuttle, *J. Am. Ceram. Soc.* 79, 536 (1996).
31. J. Claus, M. Leonhardt, and J. Maier, *J. Phys. Chem. Solids* 61, 1199 (2000).
32. R.A. Eichel, *Phys. Chem. Chem. Phys.* 13, 368 (2011).
33. C. Schaffrin, *Phys. Status Solidi A* 35, 79 (1976).